An official publication of the International Society for Energy, Environment and Sustainability (ISEES)

Journal of Energy and Environmental Sustainability

Journal homepage : www.jees.in

Thermal and Thermohydraulic Performance of Double Flow Flat Plate and Corrugated Absorber Solar Air Heaters

Som Nath Saha* and S. P. Sharma

Department of Mechanical Engineering, National Institute of Technology, Jamshedpur, India

ARTICLE INFO

Received : 01 May 2017
Revised : 31 May 2017
Accepted : 09 June 2017

Keywords:
Solar air heater, double flow, corrugated absorber, thermal efficiency, thermohydraulic efficiency

ABSTRACT

In this work, thermal and thermohydraulic performance of double flow flat plate and corrugated absorber solar air heaters are analytically investigated. Three types of collectors are considered in this study, first one has flat plate absorber (SA-1), second has corrugated absorber (SA-2) and third one has corrugated absorber and bottom plates (SA-3). The aim of the use of the corrugated absorbing plate and bottom plate is to enhance the turbulence and the heat transfer rate inside the air flow channel which help to improve the performance of collector. The performance of these three types of solar air heater are analyzed on the basis of effective parameters such as mass flow rate and insolation. The results show that the corrugated absorber solar air heaters (SA-2 and SA-3) have much higher efficiencies than the flat plate solar air heater (SA-1) although performance of SA-3 collector is superior to that of SA-2 collector. The percentage enhancement in efficiency of SA-3 collector with respect to SA-1 collector is 11.86 % for the mass flow rate of 0.035 kg/s.The results also show that increasing the solar intensity leads to achieve higher air temperature rise and efficiency.

Nomenclature:

A_c **area of collector (m²)**
b Chalf height of v-groove (m)
C_p specific heat of air at constant pressure (J/kg K)
D_h hydraulic diameter (m)
f friction coefficient
h heat transfer coefficient (W/m² K)
H height of air flow channel (m)
H_{gc} height of glass cover (m)
I insolation (W/m²)
k thermal conductivity (W/m K)
L collector length (m)
m mass flow rate (kg/s)
Nu Nusselt number
Q energy gain by air (W)
R resistance factor
Re Reynolds number
T temperature (K)
U loss coefficient (W/m² K)
V velocity of wind (m/s)
v velocity of air (m/s)
W collector width (m)

Greek symbols

α absorptivity
φ emissivity
ϕ fraction of mass flow rate
ΔP pressure drop (N/m²)
η efficiency
ρ density of air (kg/m³)
τ transmissivity
θ angle of v-groove absorbing plate (⁰)

Subscripts

a ambient
ap absorber plate
B bottom
bp bottom plate
c convective
ch channel
e net
en entrance
ex exit
f total flow
f1 flow above the absorber plate
f2 flow under the absorber plate
gc glass cover
gc1 lower glass cover
gc2 upper glass cover
in inlet
max maximum
min minimum
o outlet
r radiative
T top
eff thermohydraulic (effective)
u useful

* Corresponding Author: *somnath.rvs@gmail.com*

1. Introduction

Solar energy is one of the renewable source of energy which is sustainable, abundant and clean. Among various applications of solar energy, air heating through the solar air heaters are very simple and economic. Solar air heaters are mainly used for low to medium grade thermal energy, like space heating, cooling, crop drying etc. Even though it is simple in design, low maintenance and operating cost, its efficiency is low due to poor thermo physical properties of air. To improve the performance of solar air heaters several designs are developed by many researchers. Such design includes honeycomb collectors, extended surface absorber, use of artificial roughness on the absorber plate, packing of porous material in air flow channel. One of the effective ways to improve the convective heat transfer rate is to increase the heat transfer surface area and to increase turbulence inside the channel by using fin or corrugated surfaces [Goldstein, 1976, 1977].

Ho-Ming et al. [1999] investigated the performance of double flow flat plate solar air heater and found more effective than conventional solar air heater. A parametric study of cross corrugated solar air collectors with different parameters such as mass flow rate, insolation and inlet temperature have been performed by Wenxian et al. [2006] and Wenfeng et al. [2007] and found that the cross corrugated collector have superior thermal performance than that of the flat plate. Mohammadi and Sabzpooshani [2013] investigated the influence of fins and baffles attached over the absorber plate on the performance of single pass solar air heater. Vimal and Sharma [2016] theoretically investigated the thermal performance of packed bed solar air heater with wire screen matrices. Paisarn [2005] studied numerically about heat transfer characteristics and performance of double pass flat plate solar air heater with and without porous media. A comprehensive study of solar air heater having roughness elements on the absorber plate with different geometry, presented by Mittal et al. [2007]. Karmare and Tikekar [2010] presented the analysis of fluid flow and heat transfer in a rib grit roughened surface solar air heater.

This paper present analyticaly investigations of thermal and thermohydraulic performance of double flow flat plate and corrugated absorber solar air heaters. Three types of solar air heaters are considered, SA-1 (Fig. 1a) has flat plate absorber, SA-2 (Fig. 1b) has corrugated absorber plate and SA-3 (Fig. 1c) has corrugated absorber and bottom plate having convergence-divergence flow channel.

2. Methods

2.1 Theoretical analysis

Figure 1 shows the schematic diagram of double flow solar air heater with two glass cover. The analysis is based on analytical solutions for energy balance equations. The energy balance equations are made under the following assumptions:

- Air temperature variation is the functions of the flow directions only.
- Temperature drop across the glass cover, absorber plate and bottom plate is negligible.
- The systems operate under quasi steady state.
- Glass covers and flowing air do not absorb radiant energy.

2.2 Energy Balance Equations

Considered a differential element of length dx at a distance x from the inlet. The energy balance equations are written as:

Glass cover 1 (lower glass cover)

$$h_{r,ap-gc1}(T_{ap}-T_{gc1})Wdx + h_{c,f1-gc1}(T_{f1}-T_{gc1})Wdx = U_{gc1-a}(T_{gc1}-T_a)Wdx \quad (1)$$

Absorber plate

$$I\alpha_{ap}\tau_{gc}^2 Wdx = U_T(T_{ap}-T_a)Wdx + U_B(T_{ap}-T_a)Wdx + h_{c,ap-f1}(T_{ap}-T_{f1})Wdx + h_{c,ap-f2}(T_{ap}-T_{f2})Wdx \quad (2)$$

Bottom plate

$$h_{r,ap-bp}(T_{ap}-T_{bp})Wdx + h_{c,f2-bp}(T_{f2}-T_{bp})Wdx = U_{bp-a}(T_{bp}-T_a)Wdx \quad (3)$$

Air flow 1 (air flowing over the absorbing plate)

$$h_{c,ap-f1}(T_{ap}-T_{f1})Wdx = m\varphi c_p dT_{f1} + h_{c,f1-gc1}(T_{f1}-T_{gc1})Wdx \quad (4)$$

Air flow 2 (air flowing under the absorbing plate)

$$h_{c,ap-f2}(T_{ap}-T_{f2})Wdx = m(1-\varphi)c_p dT_{f2} + h_{c,f2-bp}(T_{f2}-T_{bp})Wdx \quad (5)$$

Solving Eqs. (1) – (5), the outlet temperature of flow 1 and flow 2 are respectively as:

$$T_{f1,o} = \left[\frac{Y_1-\frac{M_5}{1-\varphi}}{\frac{M_4}{(1-\varphi)}}\right]C_1 e^{\frac{Y_1}{Z}} + \left[\frac{Y_2-\frac{M_5}{1-\varphi}}{\frac{M_4}{(1-\varphi)}}\right]C_2 e^{\frac{Y_2}{Z}} - \frac{M_5}{M_4}\left(\frac{M_3M_4-M_1M_6}{M_1M_5-M_2M_4}\right) - \frac{M_6}{M_4} + T_a \quad (6)$$

and

$$T_{f2,o} = C_1 e^{\frac{Y_1}{Z}} + C_2 e^{\frac{Y_2}{Z}} + \frac{M_3M_4-M_1M_6}{M_1M_5-M_2M_4} + T_a \quad (7)$$

Where $z = \frac{mc_p}{A_c}$

and Y's and C's are the functions of M and M's are in the terms of the convective heat transfer coefficient, loss coefficients and physical properties (Appendix A).

$$\eta = \frac{mc_p}{IA_c}(T_{f,o}-T_{f,in}) = \frac{Z}{I}\Delta T \quad (8)$$

2.3 Heat Transfer Coefficients

For flat plate absorber

The convective heat transfer coefficient for air.

$$h_{c,ap-f} = \frac{Nuk_f}{D_h} \quad (9)$$

For laminar flow, the equation presented by Heaton et al. [1964]

$$Nu = 4.4 + \frac{0.00398(0.7ReD_h/L)^{1.66}}{1+0.0114(0.7ReD_h/L)^{1.12}} \quad (10)$$

For turbulent flow the correlation derived from Kays [1980], data with the modification of McAdams [1954].

$$Nu = 0.0158Re^{0.8}[1+(D_h/L)^{0.7}] \quad (11)$$

For v-corrugated absorber

The convective heat transfer coefficient for air [2014]

$$h_{c,ap-f} = \frac{Nuk_f}{D_h} \times \frac{1}{sin\left(\frac{\theta}{2}\right)} \quad (12)$$

Hollands and Shewen [1981] developed the correlation of Nusselts number (N_u) and modified by Karim et al. [2014] as:

If $Re < 2800$

$$Nu = 2.821 + 0.126\,Re\frac{2b}{L} \quad (13)$$

If $2800 \le Re \le 10^4$

$$Nu = 1.9\times10^{-6}Re^{1.79} + 225\frac{2b}{L} \quad (14)$$

If $10^4 \le Re \le 10^5$

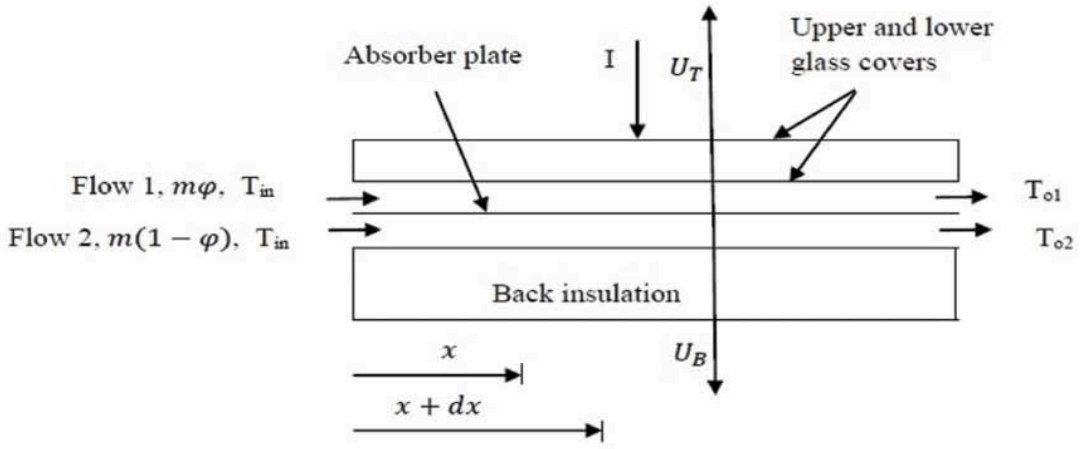

(1a)

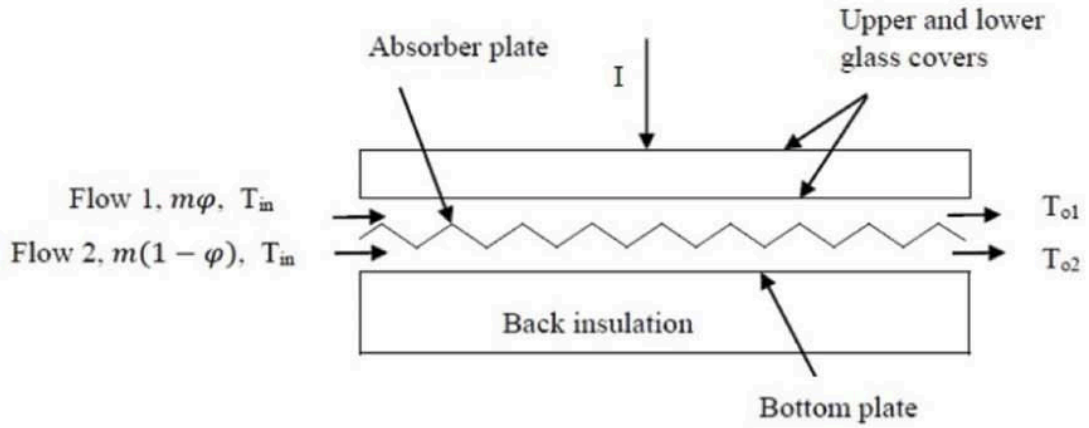

(1b)

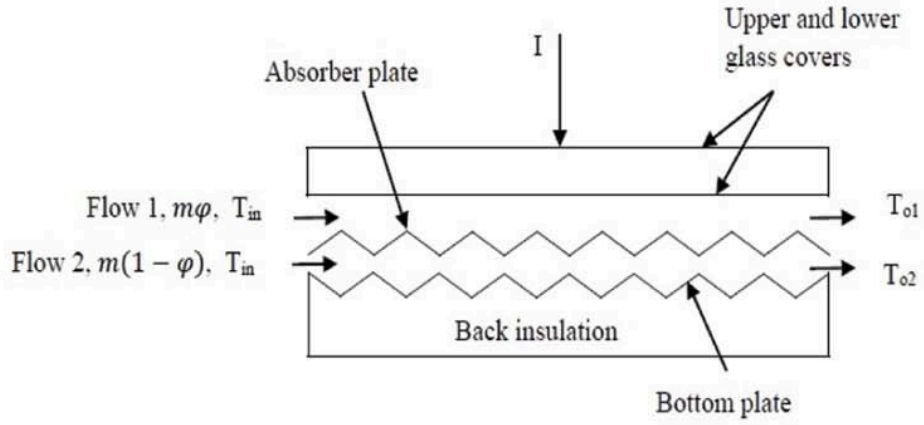

(1c)

Fig. 1. The schematic diagrams of double flow solar air heater with two glass cover; (1a) Flat plate, (1b) Corrugated absorber plate and (1c) Corrugated absorber and bottom plate

$$Nu = 0.0302Re^{0.74} + 0.242Re^{0.74}\frac{2b}{L} \quad (15)$$

For v-corrugated absorber and bottom plate
Benli [2013] present the correlation of Nusselts number as:

Nu = 0.5999Re$^{0.419}$

$$Nu = 0.5999Re^{0.419} \quad (16)$$

2.4 Thermohydraulic Efficiency

The net energy can be written as:

$$Q_e = Q_{uf} - P_m/C_f \quad (17)$$

where P_m is the work energy lost in friction in the heater channel, given by:

$$P_m = m\Delta P/\rho \quad (18)$$

C_f is the conversion factor to transform different efficiencies (thermal to mechanical) and is taken 0.2 [Bahrehmand, 2015].

The pressure drop ΔP is calculated from the following expression;

$$\Delta P = \Delta P_{ch} + \Delta P_{en} + \Delta P_{ex} \quad (19)$$

The pressure drop through the upper and lower channel ΔP_{ch} is calculated by the relation [Wong, 1977; Choudhury, 1988; Tan, 1969];

$$\Delta P_{ch} = 2\rho v_{ch}^2 fL/D_h \quad (20)$$

The friction factor is given by [Wong, 1977; Choudhury, 1988; Tan, 1969; Douglas, 1992]; for turbulent flow

$$f = 0.059Re^{-0.2} \quad (21)$$

for laminar flow

$$f = 16/Re \quad (22)$$

The friction factor for SA-3 is given by [Benli, 2013];

$$f = 1.0866Re^{-0.6635} \quad (23)$$

The sum of the inlet and outlet pressure drop (ΔP_{en} + ΔP_{ex}) can be determined by Hegazy [2000];

$$\Delta P_{en} + \Delta P_{ex} = (R_{en} + R_{ex})\frac{\rho v_p^2}{2} \quad (24)$$

where the sum of the entrance and exit resistance factor (R_{en} + R_{ex}) is taken 1.5 [Griggs, 1992].

The thermohydraulic efficiency of the solar air heater can be expressed as;

$$\eta_{eff} = \frac{Q_e}{A_c I} = \frac{Q_{uf} - (P_m/C_f)}{A_c I} \quad (25)$$

3. Results and discussion

In this section, results of thermal and thermohydraulic performance of double flow flat plate and corrugated absorber solar air heaters are presented. The following values are used for the parameters under the typical configuration and operating conditions:

L = 1.25 m, W = 0.80 m, H_{gc} = 0.025 m, H_{min} = 0.02 m, H_{max} = 0.045 m, τ_{gc} = 0.875, α_{ap} = 0.96, ε_{gc} = 0.94, ε_{ap} = 0.80, ε_{bp} = 0.94, $U_B \simeq 0$, T_a = 30 °C = 303 K, V = 1 m/s, b = 0.00625 m, I = 200 – 1000 W/m^2, m = 0.014 – 0.083 kg/s, φ = 0.5.

Figure 2 shows the variation of air temperature rise with mass flow rate for double flow flat and corrugated absorber solar air heaters for I = 1000 W/m^2. Air temperature rise continuously decreases with increase in mass flow rate for all solar air heaters. It is seen from the figure that the considerable amount of gain in air temperature rise at lower mass flow rate is observed due to corrugated absorber and at higher mass flow rate air temperature rise of all collectors are almost same. The maximum value of air temperature rise is 18.9^{0}C for SA-1, 20.8^{0}C for SA-2 and 21.2^{0}C for SA-3 at m = 0.035 kg/s.

Figure 3 shows the composite plot of thermal and thermohydraulic efficiencies as a function of mass flow rate of various types of double flow solar air heaters for I = 1000 W/m^2. From the figure it is clearly seen that thermal efficiency increases continuously with increase in mass flow rate, whereas thermohydraulic efficiency increases upto a certain mass flow rate of each collector and then gradually decreases. It is also indicated that the peak value of thermo hydraulic efficiency of double flow flat plate solar air heater (SA-1) reaches maximum value at m = 0.0575 kg/s, whereas for SA-2 and SA-3 collectors pick values of thermohydraulic efficiency shifted towards lower mass flow rates of 0.0475 kg/s and 0.046 kg/s respectively. This type of trends is observed due to increase in pressure drop of flowing air in case of corrugated absorber / channels.

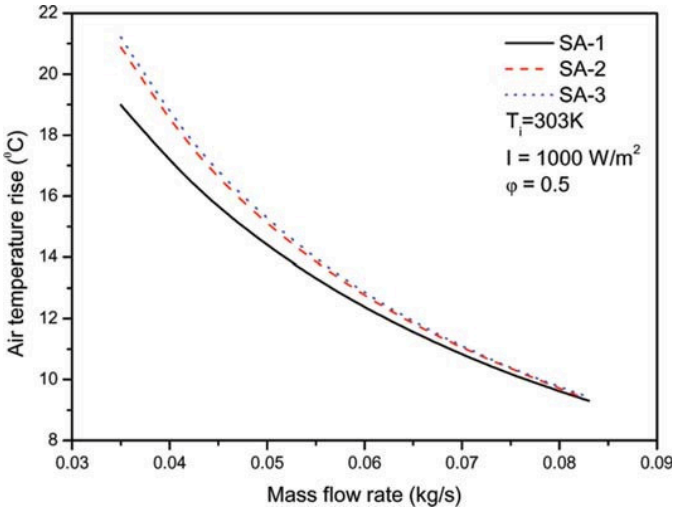

Fig. 2. Air temperature rise vs. mass flow rate

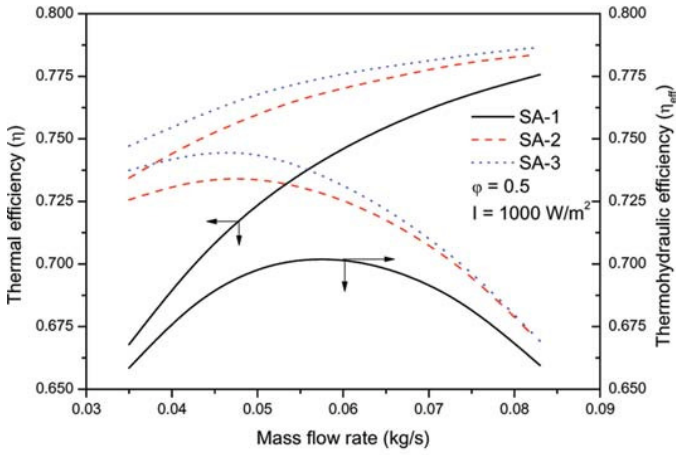

Fig. 3. Thermal and Thermohydraulic efficiency vs. mass flow rate

The percentage enhancement in both thermal as well as thermo hydraulic efficiency is higher at lowest mass flow rate and goes on decreasing with increase in mass flow rate and almost negligible at highest mass flow rate of 0.083 kg/s.

The variation of air temperature rise with insolation, for flat plate and corrugated absorber collectors for m = 0.042 kg/s, are shown in Fig. 4. It evident that air temperature rise increase linearly with increase in insolation. It is also evident from the figure that corrugated absorber collectors have higher air temperature rise to the flat plate collector. The maximum air temperature rise is 16.5^{0}C at I = 1000 W/m^2 for SA-3 collector.

Figure 5 shows the variation of efficiency as a function of insolation at m= 0.042kg/s for a set of parameters. The efficiency increase with increase in insolation for all collectors. Figure also reveals that the SA-2 and SA-3 collectors have much higher efficiency than the flat plate collector (SA-1) and SA-3 collector performs superior to the SA-2 collector for all the values of insolation considered. This is because of increase in turbulence of air flow leads to increase convective heat transfer rate.

Figure 6 shows the effect of insolation on thermohydraulic efficiency for m = 0.042 kg/s. It can be observed that thermohydraulic efficiency monotonically increases with increase in insolation then a slight fall is observed in the rate of increase of thermo hydraulic efficiency as insolation increases due to at lower insolation heat gain is low and at high insolation heat gain is high. The maximum thermohydraulic efficiency is 74.25 % at I = 1000 W/m^2 for SA-3 collector.

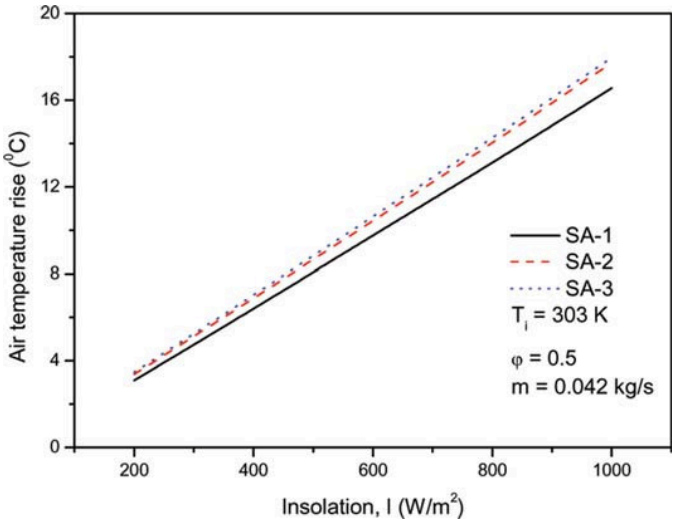

Fig. 4. Air temperature rise vs. insolation

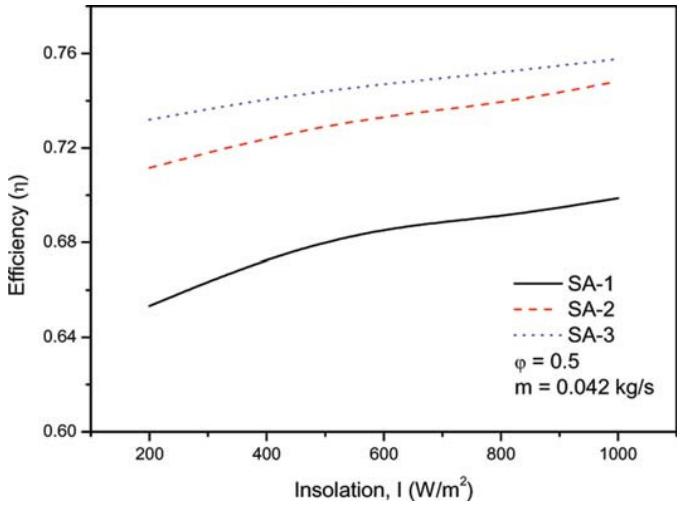

Fig. 5. Efficiency vs. insolation

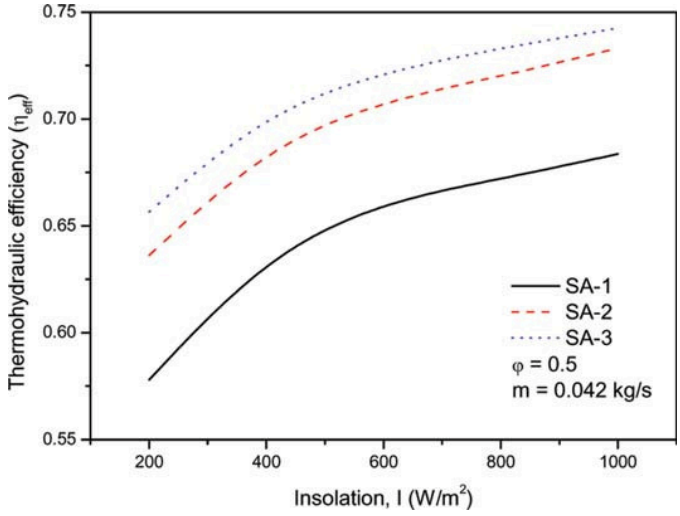

Fig. 6. Thermohydraulic efficiency vs. insolation

4. Conclusions

In this study, thermal and thermohydraulic analysis of double flow flat plate and corrugated absorber solar air heaters as a function of different parameters such as mass flow rate and insolation have been performed. Results indicated that the air temperature rise decreases while efficiency increases with increase in mass flow rate. It is observed that thermohydraulic efficiency increases upto a certain limit of mass flow rate and there after it decreases. The SA-3 solar air heater attains maximum value of thermohydraulic efficiency at air mass flow rate of 0.046 kg/s. There is significant enhancement in air temperature rise and efficiency of double flow corrugated absorber to that of the flat plate absorber solar air heater. For a specific mass flow rate air temperature rise, efficiency and thermohydraulic efficiencies are increases with increase in insolation.

References

Bahrehmand D, Ameri M,Gholampour M, 2015. Energy and exergy analysis of different solar air collector systems with forced convection, Renewable Energy, 83, 1119-1130.

Benli H, 2013. Experimentally derived efficiency and exergy analysis of a new solar air heater having different surface shapes, Renewable Energy, 50, 58-67.

Choudhury C, Andersen SL Pekstad J, 1988. A solar air heater for low temperature applications, Solar Energy, 40, 77.

Douglas JF, Gasiorek JM,Swaffield, JA, 1992. Fluid mechanics, 2nd ed. England: Longman Singapor Publishers.

Goldstein L, Sparrow E.M, 1976. Experiments on the transfer characteristics of a corrugated fin and tube heat exchanger configuration, Transaction of the ASME, Journal of Heat Transfer, 98, 26-34.

Goldstein L, Sparrow EM, 1977. Heat/mass transfer characteristics for flow in a corrugated wall channel, Transaction of the ASME, Journal of Heat Transfer,99, 187-195.

Griggs EI,Sharifabad FK, 1992. Flow characteristics in rectangular ducts, ASHRAE Trans, 98(1), 116-27.

Heaton HS, Reynolds Wc., Kays W.M., 1964. Heat transfer in annular passages. Simultaneous development of velocity and temperature fields in laminar flow,Int J Heat Mass Transfer, 7, 763-81.

Hegazy AA, 2000. Thermohydraulic performance of air heating solar collectors with variable width, flat absorber plates, Energy Convers Manage, 41, 1361-78.

Hollands KGT,Shewen EC, 1981. Optimization of flow passage geometry for air heating plate type solar collectors, ASME J Solar Energy Eng, 103, 323-30.

Ho-MingYeh, Chii-Dong Ho, Jun-ZeHou, 1999. .The improvement of collector efficiency in solar air heaters by simultaneously air flow over and under the absorbing plate, Energy, 24, 857-871.

Karim MA, Perez E, Amin ZM, 2014. Mathematical modelling of counter flow v-grove solar air collector, Renewable Energy, 67, 192-201.

Karmare SV,Tikekar AN, 2010. Analysis of fluid and heat transfer in a rib roughened surface solar air heater using CFD, Solar Energy, 84, 409-17.

Kays WM, 1980. Convective heat and mass transfer, New York, McGraw Hill.

McAdams WH, 1954. Heat transmission, New York, McGraw-Hill.

Mohammadi K, Sabzpooshani M, 2013. Comprehensive performance evaluation and parametric studies of single pass air heater with fins and baffles attached over the absorber plate, Energy,57, 741-750.

Mittal MK, Varun Saini RP,Singal SK, 2007. Effective efficiency of solar air heaters having different types of roughness element on the absorber plate, Energy, 32, 739-745.

PaisarnNaphon, 2005. Effect of porous media on the performance of the double pass flat plate solar air heater, International Communications in Heat and Mass Transfer, 32, 140-150.

Tan HM, Charters WWS, 1969. Effect of thermal entrance region on turbulent forced convective heat transfer for an asymmetrically heated rectangular duct with uniform heat flux, Solar Energy, 12, 513.

Vimal KuChouksey, Sharma SP, 2016. Investigations on thermal performance characteristic of wire screen packed bed solar air heater, Solar Energy, 132, 591-605.

Wenxian Lin, Wenfeng Gao, Tao Liu, 2006. A parametric study on the thermal performance of cross corrugated solar air collectors, Applied Thermal Engineering, 26, 1043-53.

WenfengGao, Wenxian Lin, Tao Liu,Chaofeng Xia, 2007. Analytical and experimental studies on the thermal performance of cross corrugated and flat pate solar air heaters, Applied Energy, 84, 425-441.

Wong HY, 1977. Handbook of essential formula and data on heat transfer for engineers, London: Longman.

Appendix A

$$J_1 = \frac{U_T+U_B+h_{c,ap-f2}}{U_T+U_B+h_{c,ap-f1}+h_{c,ap-f2}} \quad (A.1)$$

$$J_2 = \frac{h_{c,ap-f2}}{U_T+U_B+h_{c,ap-f1}+h_{c,ap-f2}} \quad (A.2)$$

$$J_3 = \frac{I\alpha_{ap}\tau_{gc}^2}{U_T+U_B+h_{c,ap-f1}+h_{c,ap-f2}} \quad (A.3)$$

$$J_4 = \frac{1}{h_{r,ap-gc1}+h_{c,f1-gc1}+U_{gc1-a}} \quad (A.4)$$

$$J_5 = \frac{U_T+U_B+h_{c,ap-f1}}{U_T+U_B+h_{c,ap-f1}+h_{c,ap-f2}} \quad (A.5)$$

$$J_6 = \frac{h_{c,ap-f1}}{U_T+U_B+h_{c,ap-f1}+h_{c,ap-f2}} \quad (A.6)$$

$$J_7 = \frac{1}{h_{r,ap-bp}+h_{c,f2-bp}+U_{bp-a}} \quad (A.7)$$

$$M_1 = -J_1h_{c,ap-f1} - J_4h_{c,f1-gc1}U_{gc1-a} - J_1J_4h_{c,f1-gc1}h_{r,ap-gc1} \quad (A.8)$$

$$M_2 = J_2h_{c,ap-f1} + J_2J_4h_{c,f1-gc1}h_{r,ap-gc1} \quad (A.9)$$

$$M_3 = J_3h_{c,ap-f1} + J_3J_4h_{c,f1-gc1}h_{r,ap-gc1} \quad (A.10)$$

$$M_4 = J_6h_{c,ap-f2} + J_6J_7h_{c,f2-bp}h_{r,ap-bp} \quad (A.11)$$

$$M_5 = -J_5h_{c,ap-f2} - J_7h_{c,f2-bp}U_{bp-a} - J_5J_7h_{c,f2-bp}h_{r,ap-bp} \quad (A.12)$$

$$M_6 = J_3h_{c,ap-f2} + J_3J_7h_{c,f2-bp}h_{r,ap-bp} \quad (A.13)$$

$$Y_1 = \frac{1}{2}\left[\left(\frac{M_1}{\varphi}+\frac{M_5}{(1-\varphi)}\right) + \sqrt{\left(\frac{M_1}{\varphi}-\frac{M_5}{(1-\varphi)}\right)^2+\frac{4M_2M_4}{\varphi(1-\varphi)}}\right] \quad (A.14)$$

$$Y_2 = \frac{1}{2}\left[\left(\frac{M_1}{\varphi}+\frac{M_5}{(1-\varphi)}\right) - \sqrt{\left(\frac{M_1}{\varphi}-\frac{M_5}{(1-\varphi)}\right)^2+\frac{4M_2M_4}{\varphi(1-\varphi)}}\right] \quad (A.15)$$

$$C_1 = -\left[\left(\frac{\frac{M_4}{1-\varphi}+\frac{M_5}{1-\varphi}-Y_2}{Y_2-Y_1}\right)(T_{f,in}-T_a) + \left(\frac{Y_2}{Y_2-Y_1}\right)\left(\frac{M_3M_4-M_1M_6}{M_1M_5-M_2M_4}\right) + \frac{\frac{M_6}{1-\varphi}}{Y_2-Y_1}\right] \quad (A.16)$$

$$C_2 = \left(\frac{\frac{M_4}{1-\varphi}+\frac{M_5}{1-\varphi}-Y_1}{Y_2-Y_1}\right)(T_{f,in}-T_a) + \left(\frac{Y_1}{Y_2-Y_1}\right)\left(\frac{M_3M_4-M_1M_6}{M_1M_5-M_2M_4}\right) + \frac{\frac{M_6}{1-\varphi}}{Y_2-Y_1} \quad (A.17)$$